*Progress In Electromagnetics Research, Vol. 149, 133–145, 2014*

# A Satellite Multiple-Beam Antenna for High-Rate Data Relays

**Lukasz A. Greda[1, *], Andreas Winterstein[1], Achim Dreher[1], Sascha A. Figur[2], Bernhard Schoenlinner[2], Volker Ziegler[2], Marco Haubold[3], and Martin W. Brueck[4]**

**Abstract**—This paper describes the concept and the development of key components of a novel multiple-beam antenna for satellite applications. The antenna is designed to be used in a transparent high-rate data relay system that links several low earth orbit (LEO) satellites to a single ground station via a satellite positioned on a geostationary orbit (GEO). The proposed antenna is based on the concept of an array-fed reflector. The antenna can track LEO satellites by switching between different subarrays of a bigger multifeed array using a reconfigurable switch matrix based on radio frequency micro-electro-mechanical system (RF MEMS) switches. The radiation characteristic of the antenna is further improved by combining digital beamforming with beam switching. In order to validate the proposed antenna concept and to show its suitability for space applications a demonstrator has been built. Measurements of the antenna's key components and of the demonstration system are given.

## 1. INTRODUCTION

The recently launched LEO satellites for earth observation purposes are equipped with powerful scientific instruments that can acquire tremendous amounts of data. Downloading all gathered data to earth is becoming an increasingly serious bottleneck. The main problem is the relatively short span of time (typically 10 min.) during which a single ground station can receive data from a passing LEO satellite. An elegant way to circumvent this bottleneck is the utilization of a GEO satellite to redirect high data rate LEO signals to an earth station (see Fig. 1), since the majority of LEO satellites is visible to a GEO satellite for at least 50% of their orbital period. For typical LEO earth observation satellites moving on polar orbits, GEO data relays offer access times about a factor of 15 higher than a direct link to a single ground station could provide. This increase in contact time can be utilized to enhance the transmitted data throughput and/or to reduce the data rate requirements.

Another advantage of the concept described here is that even simultaneous data link communication from multiple LEO satellites to one GEO satellite becomes feasible, if a suited multiple-beam antenna is used on the GEO satellite. This feature distinguishes the proposed concept from the existing data relay systems in Ka-band like NASA TDRS system [1]. High-rate data transfer from a LEO satellite to a GEO satellite calls for a high-gain link that is only achievable if steerable directive antennas on both sides are utilized. Instead of equipping many LEO satellites with large transmit antennas, it is advantageous to realize the receiving antenna with higher gain, thus relaxing requirements for aperture and transmit power of the LEO antennas. To cover most of the LEO orbits, an antenna located on a GEO satellite must have a scan angle of at least $\pm 10^\circ$. The beamwidth should not exceed $1^\circ$ to allow spatial filtering ability of the antenna without significant impairment. Two basic architectures of electronically steerable antennas with high gain and multiple-beam capability can be identified: the direct radiating array (DRA) and the array-fed reflector [2]. In the open literature some examples of active satellite phased-array antennas with multiple-beam capability can be found [3–5]. However, these solutions have too low gain and too small scan volume to be used for GEO data relays. Realizing

*Received 25 July 2014, Accepted 15 September 2014, Scheduled 13 October 2014*

* Corresponding author: Lukasz A. Greda (lukasz.greda@dlr.de).

[1] German Aerospace Center (DLR), Institute of Communications and Navigation, Oberpfaffenhofen, Wessling 82234, Germany. [2] Airbus Defence and Space GmbH, Airbus Group Innovations, Munich 81663, Germany. [3] Fraunhofer ENAS, Chemnitz 09126, Germany. [4] SINTEC Microwave Systems GmbH, Boeblingen 71034, Germany.

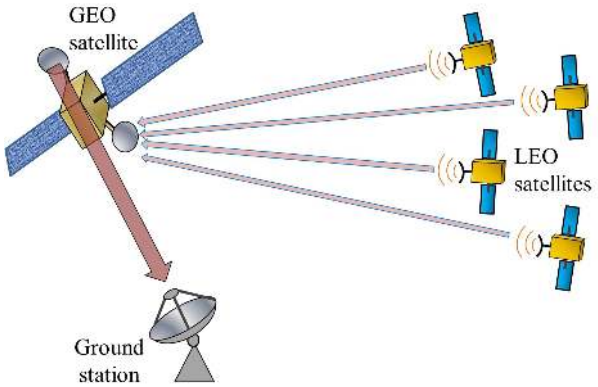


**Figure 1.** Concept of the high-rate data relay between a GEO satellite and several LEO satellites.

the required gain and scan volume with the DRA antenna alone would lead to a very high number of antenna elements resulting in excessively high complexity of the corresponding control logic. Reducing the number of required array elements by increasing the distance between them can only be done to a certain extent, as grating lobes that appear in the field of view of the antenna quickly limit the scan region. A more adequate solution for GEO data relays seems to be the array-fed reflector, since the needed high gain is obtained through the aperture of the reflector. This allows using an array of feeds having considerably fewer elements than a comparable DRA would require. Array-fed reflectors can track moving satellites by switching between different array elements. This way the gain profile of the antenna and thus the achievable data rate can significantly fluctuate. To raise these gain minima digital beamforming [6], will be deployed on the level of sub-arrays. Using adaptive beamforming for array-fed reflectors allows also for compensation of pointing errors, tolerances and suppression of interferers [7, 8]. This paper provides an overview of the whole concept of the satellite multiple-beam antenna for high-rate data relays, the development of its key components and a demonstration system built to validate the proposed design. Some parts of the work presented here were already published in [9–15]. The next section presents the concept of the proposed antenna for high-rate data relays that combines beam switching with digital beamforming. The antenna key components are characterized and their simulated performance is provided and discussed. Section 3 describes the built up antenna demonstrator that validates the antenna concept. Measurements of key components and the whole performance of the demonstration system are given. Finally, in Section 4 conclusions are drawn about the applicability of the proposed antenna to serve as a key component for multiple high-rate GEO data relays.

## 2. CONCEPT OF THE ANTENNA

The multiple-beam antenna concept presented here is based on the projection of signals transmitted from LEO satellites under varying angles into the direction of the GEO satellite onto different locations on the feed array (Fig. 2). There are various types of curved reflector antennas: centered and offset, single- or multi-reflector. Due to harsh environment is space it is favorable to at least partially protect the array of feeds inside the satellite. Therefore, either a dual reflector (e.g., Cassegrain) or single offset reflector antennas are preferred. Fig. 2 shows an offset single reflector arrangement that enables to attach the array of feeds to the satellite surface. While the top layer of the array is aligned with the satellite surface, the underlying layers with the active components are accessible from inside the satellite allowing the control of their temperature. The output signals of each antenna of the multifeed array first pass low noise amplification (LNA) stage integrated into the multifeed array (not explicitly shown). The outputs of the LNAs are directed to a reconfigurable switch matrix located behind the multifeed array. The switch matrix, which connects the subset of patches receiving an inter-satellite-link (ISL) signal to the transponder front-ends and signal processing electronics, will be implemented in RF MEMS technology [10], which is very advantageous due to its low losses and its inherent low power consumption.

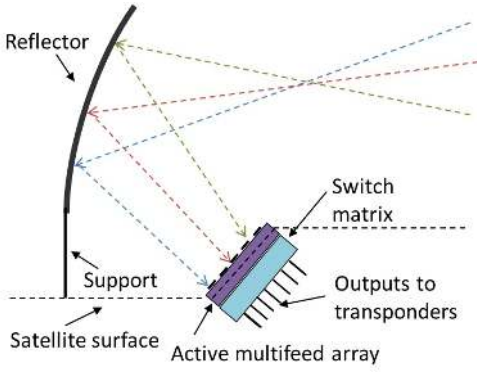


**Figure 2.** Proposed array-fed reflector antenna in offset configuration.

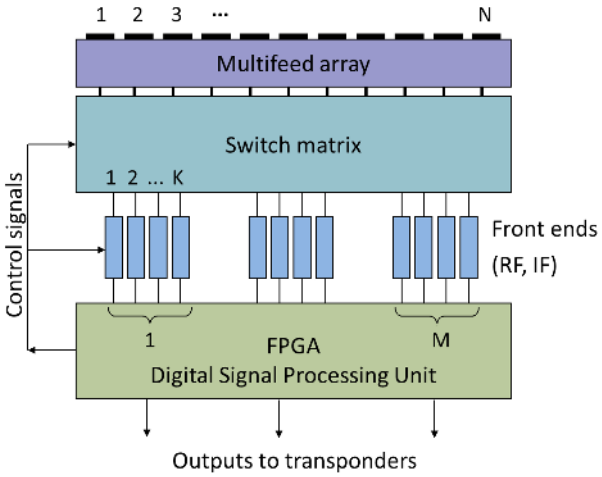


**Figure 3.** Proposed beamforming concept.

As already mentioned, LEO satellites can be tracked by switching between different beams. However, the antenna gain can fluctuate significantly in such a case, as the tracked satellite moves from one beam to another. The amount of this gain variance depends on the beamwidth and the distance between the elements. Decreasing the distance between the multifeed array elements leads certainly to a rise of the gain minima at the transition point from one beam to another. However, it results also in a much higher number of feed elements and thus complexity of the whole antenna system as well as in an increased mutual coupling between the elements. The uniformity and smoothness of the receiving gain of the multiple-beam antenna can be further optimized, if the direction of each beam can be electronically steered to a sufficient extent. This can be accomplished by the additional use of a suited beamforming technique. Fig. 3 shows a schematic view of the proposed beamforming concept.

The multifeed array has N elements from which the switch matrix simultaneously transmits signals of M beams, i.e., receives data from M LEO satellites in parallel. Each beam is generated by K array elements that are denoted in this paper as subarrays. Each array element can be a single antenna (e.g., patch) or a small array with its own fixed feed network. For each beam, the beamforming coefficients are computed separately and applied in each case to K elements resulting in steering the beam to the desired direction or beam shaping to obtain the best possible reflector illumination and therefore the maximal possible directivity of the whole antenna. In the case when the positions of the GEO and LEO satellites are exactly known, the excitation coefficients can be computed in a deterministic way. However, better results can be achieved using adaptive beamforming, as it allows to compensate for pointing errors, tolerances and to suppress interferers [7, 8]. Even when signals from several satellites are received in parallel, only a small part of the multifeed array is involved in the data reception. The remaining majority of the multifeed array can be switched-off, as each subarray possesses its own low noise amplifier integrated into the multifeed array. Thus, comparing to the DRA precious power on the satellite can be saved. In the following subsections the main components of the antenna are described and their simulated performance is discussed.

### 2.1. Array-Fed Reflector

Array-fed reflectors suffer from larger scan losses than direct radiating arrays. This is very disadvantageous for the proposed application because LEO satellites are seen by a GEO satellite during large parts of their visibility periods at high angles. The preliminary numerical simulations of scanning capabilities of the offset single reflector antenna presented in [9] show scan losses of almost 10 dB at the edge of the coverage (steering angles of about 10°). Therefore, the effectively achievable data rate was significantly reduced. Scan losses can be improved by increasing focal length-to-diameter (F/D) ratio.

If thereby the length of the antenna exceeds the available stowage area on the satellite, more compact solutions such as front-fed offset Cassegrain or side-fed offset Cassegrain can be employed [16, 17].

For covering the scan angle of $\pm 10^\circ$ and generating beamwidth smaller than one degree, the array of feeds must contain several hundreds of elements and be preferably of hexagonal or octagonal shape. The feeds can principally be realized in any space suitable technology (e.g., metallic horns). We propose building the multifeed array in microstrip technology as it is lightweight, cost efficient and allows for easy integration of small MMIC low noise amplifiers into the antenna structure. Possibilities for employing microstrip technology for satellite applications have been investigated for several years [18] and some practical solutions can be already found in existing satellites [19]. Fig. 4 shows simulated scanning capabilities in the principal planes of a sample offset single reflector configuration with a reflector diameter of 120 cm, F/D ratio of 1.5 and an offset angle of 25°. The reflector feed consists of a large number of patch antennas with 8 mm ($0.7\lambda$) inter-element spacing. Groups of four patches are connected by a fixed feeding network and form an antenna element. Thus, the distance between antenna elements is $1.4\lambda$. In the presented simulations, the reflector is always fed by subarrays of $2 \times 2$ antenna elements (i.e., 16 patches).

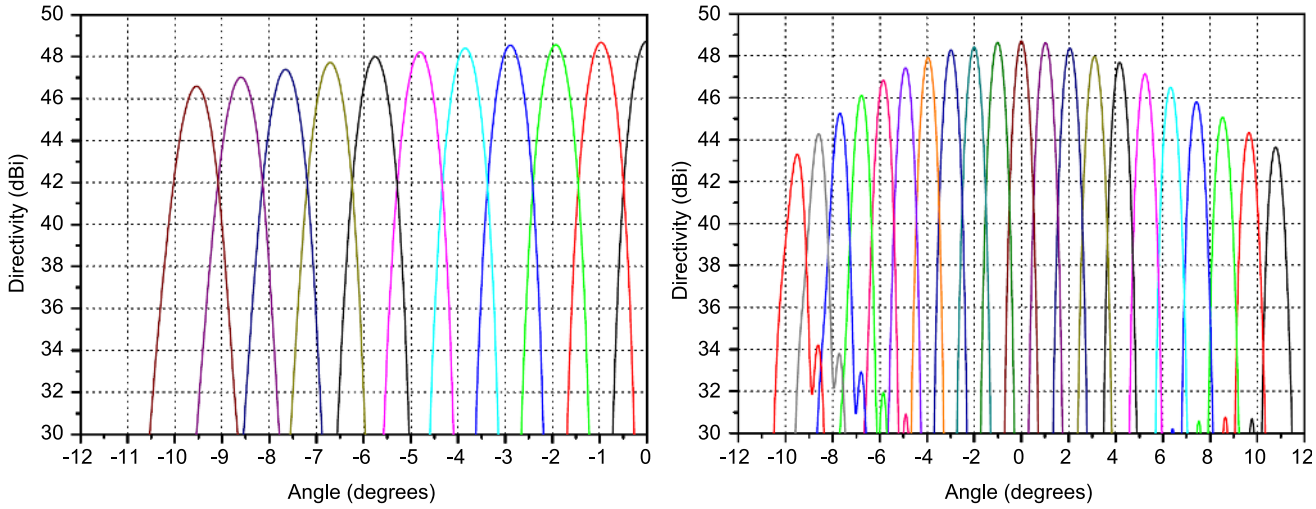


**Figure 4.** Scanning capabilities of the offset single reflector antenna. No overlapping of $2 \times 2$ subarrays. (a) Reflector symmetry plane. (b) Reflector asymmetry plane.

The simulations were performed using commercial software *FEKO* for the ISL frequency of 26 GHz employing the physical optics method combined with full ray-tracing. With the available computational resources it was not possible to model the complete feeder. Therefore, a $2 \times 2$ antenna element array composed of 16 sequentially rotated circularly polarized patches was simulated separately using *Ansys Designer* and the resulting far-field was imported to *FEKO* as a field source. To fully cover the scan angle of $\pm 10^\circ$ with the aforementioned antenna, 1380 antenna elements are necessary. In the simplest case, $2 \times 2$ subarrays are formed by hard-wiring four neighboring antenna elements to one output. The system complexity reduces to 345 outputs, but each antenna element belongs to one fixed subarray that cannot be changed. Gain fluctuations between peaks of adjacent beams can reach up to 10 dB as can be seen in Fig. 4. If an antenna element can be used for building different adjacent $2 \times 2$ subarrays then a certain spatial overlapping between the subarrays occurs. This overlapping does not mean that antenna elements can be used for different subarrays in parallel, but that at a time they can be parts of one of various subarrays. This increases system complexity but provides a finer beam grid in that the number of available beams in each direction doubles. Fig. 5 shows the improved scanning capabilities of the antenna in the case of overlapping subarrays. The gain fluctuations between two adjacent beams are decreased to approx. 3 dB. These residual fluctuations can further be minimized by beamforming.

To change the steering direction of the reflector antenna for a certain subarray, the phase center

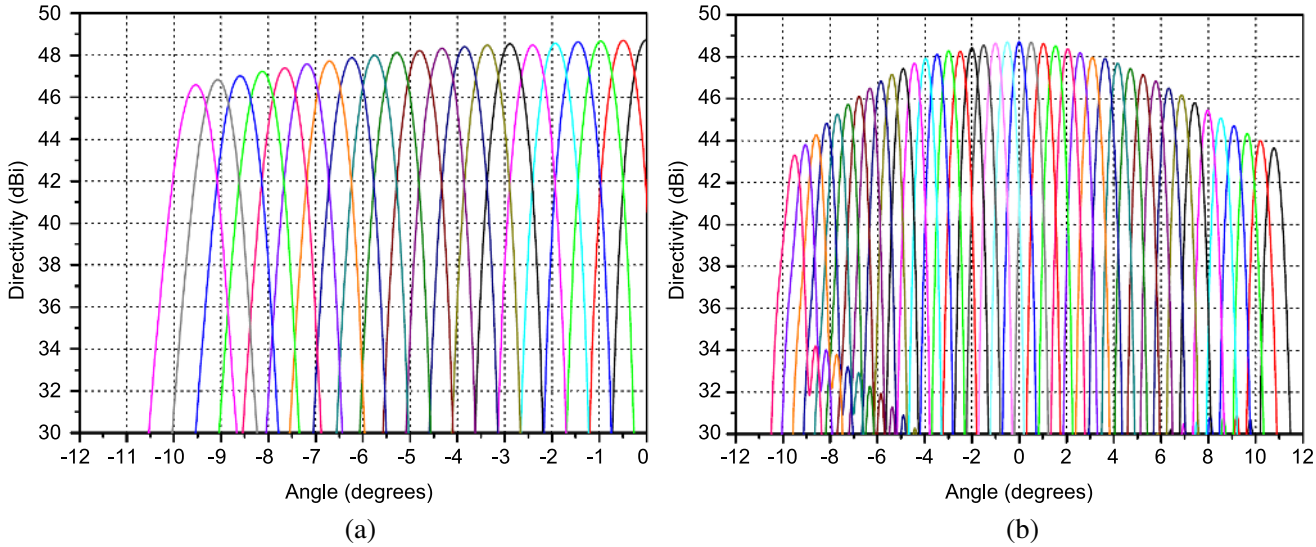


**Figure 5.** Scanning capabilities of the offset single reflector antenna. Overlapping of $2 \times 2$ subarrays. (a) Reflector symmetry plane. (b) Reflector asymmetry plane.

of the subarray must be shifted. For this purpose, at least one of the following conditions must not be fulfilled: symmetrical amplitude distribution and symmetrical or anti-symmetrical phase distribution. It must be noted that changing the pointing direction of the reflector antenna by applying beamforming to its feed elements can be done only in a relatively small region [11]. An antenna with the aforementioned parameters would be able to receive data from a LEO satellite orbiting at the altitude of roughly 500 km and equipped with a parabolic antenna with 40 cm diameter and 50 W transmit power with an average data rate of 32 Mbps in the case without overlapping and 68 Mbps in the case of digital beamforming. It would result for near-polar LEO orbit in downloadable data volumes per pass of 165 Gbits and 239 Gbits, respectively [12]. Depending on the mission's requirements and constraints, the described concept can be scaled to provide required data rates and optimized for more compact mechanical packaging for minimum stowage.

### 2.2. Switch Matrix

The switch matrix located between outputs of the multifeed array and RF front-ends is one of the major and most complex components of the proposed multiple-beam antenna system. It connects the antenna elements, which are currently in use for data transfer, to the RF front-ends for amplification, frequency down-conversion, and further signal processing. There are a number of constraints which make the design of the switch matrix a challenging task. First of all, the high number of inputs makes the system very complex. In addition, the switch matrix deals with RF-signals at around 26 GHz. Even though it is implemented after the first LNA integrated into the multifeed antenna structure, signal loss is an important design parameter. Since the system is meant for a space-borne application, size, weight, and power consumption are crucial parameters. The core functionality needed to realize a switch matrix is a multi-throw switch for RF-signals, in the most basic case a single-pole double-throw (SPDT) switch. There are a number of technologies available for switching RF-signals: coaxial switches, FETs, PIN diodes, and RF MEMS among others. Coaxial switches can be excluded for the intended application due to their bulkiness and large weight. FETs can be integrated on printed circuit boards (PCB) and compact circuits can be realized, but in general, at 26 GHz, their signal loss is not acceptable for this complex application. PIN diodes are as compact as FETs and their loss performance is better, but PIN diodes require a considerable amount of DC-current for control, which is a severe disadvantage for space-borne applications. The technology which promises lowest signal loss, compactness, low weight, and low DC-power consumption at the same time is RF MEMS.

In the case of the example antenna configuration without beamforming given in the previous section,

the switch matrix must have 345 inputs. If the antenna should support data reception from eight LEO satellites in parallel, the switch matrix must have eight outputs, each corresponding to a separate beam. For such a complex structure it is favorable to divide the matrix into several modules, thus allowing for easier fabrication and testing. It is advantageous to choose the number of inputs/outputs to be a power of two, e.g., four, eight, or 16. Complexity of the switch matrix can also be reduced by using switches with one input port and several output ports (SPxTs) integrated in a common package. Fig. 6 shows a possible modular configuration of a switch matrix with 345 inputs and eight outputs.

The 345 inputs from the antenna are connected to 22 sub-modules (type A) with 16 inputs and eight outputs, each, where each sub-module of type A has all degrees of freedom to route up to eight signal paths in any combination. The $22 \times 8$ (176) output ports from the sub-modules of type A are connected to eight sub-modules of type B with 22 input ports and one output port, each; i.e., sub-module type B is a SP22T switch. With this concept, each combination of eight antenna inputs can be routed to the eight output ports of the SP22Ts. The feasibility of the realization of such sub-modules, in particular single-pole-multi-throw switches of the aforementioned order has been proven in literature [22, 23]. For the case of the multiple-beam antenna using beamforming with four elements, the number of inputs and outputs of the switch matrix increases fourfold. This, in general, increases complexity not only by a factor of four but exponentially. However, the fact that always four adjacent antenna elements in a $2 \times 2$ configuration will act together to form a single antenna beam reduces the complexity considerably. It is possible to obtain the required functionality by providing only four times the structure of the case without digital beamforming. A considerable number of different RF MEMS concepts have been developed in the last 20 years [22–24]. So far, reliability has proven to be the most important challenge that must be solved in order for a technology to become a product. In consequence, at this point of time, only one single company produces RF MEMS switches which work beyond 26 GHz and the switches are offered only in SPDT configuration. For this project, a technology which is being developed by EADS Innovation Works was selected [13] (see Fig. 7) because of its high concept-inherent reliability and temperature stability, the demonstrated RF-performance parameters and the design flexibility offered.

The RF MEMS switch concept relies on a fixed-free curled cantilever which is implemented as series element in a microstrip line. It is separated from a high resistivity silicon substrate material by thermally grown silicon oxide. Actuation is achieved by applying a DC-voltage to the cantilever with respect to the silicon bulk material. Low-loss transmission with the cantilever in the down-state is possible through a conductive zone just below the silicon oxide in the area of the tip of the cantilever. With the cantilever in the up-state, high isolation is achieved and the switch is in the off-state.

The packaging of the RF MEMS devices was performed on four inch wafer-level as a MEMS

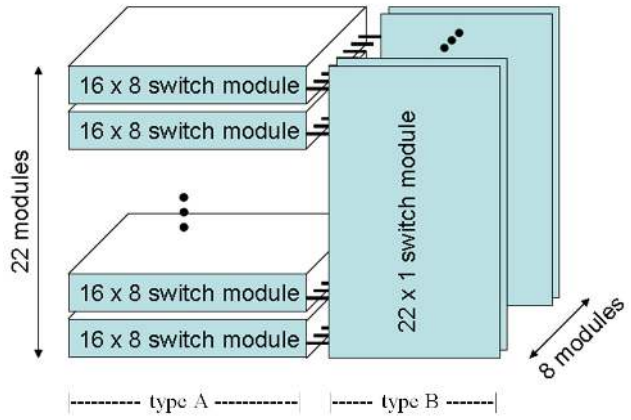


**Figure 6.** Schematic of the switch matrix concept for 345 input ports (left) and eight output ports (right). It consists of 22 16 × 8 switch matrix sub-modules connected to eight SP22T sub-modules. No beamforming is applied here.

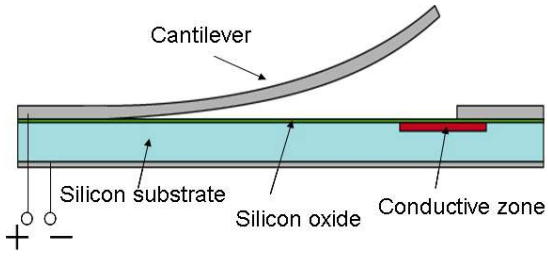


**Figure 7.** A cross-sectional view of the EADS RF MEMS switch concept.

first approach. Borofloat glass wafers were chosen as cap material since the material's coefficient of thermal expansion (CTE) is well adapted to silicon and the transparency for visual light ensures an optical characterization of the encapsulated cantilever. The main challenge for the applied technology consisted in the minimization of thermal impact on the switch element during the bonding process in terms of maximum process temperature and duration. Hence the maximum temperature was set to 210°C for approximately 30 minutes. Consequently, several technologies were not applicable such as glass frit bonding, metal based thermo-compression bonding or conventional anodic bonding [20]. Since the fabrication processes for the switch patterning and releasing cause inevitable contaminations on the wafers surface, direct bonding of silicon to glass was not applicable in addition. To meet those requirements, an adhesive bonding process with patterned SU-8 was chosen. This UV sensitive polymer allows for the production of bonding features with a height up to several hundred microns by spin coating and lithography process. It is characterized by a high mechanical, chemical and thermal stability [21]. Fig. 8 shows fabricated SPST and SP4T switch elements after final dicing process. The visual inspection of the bonding structures showed a high quality bonding with no defects. Hence, no condensed moisture was found inside the cavity after dicing. The functional testing supported the good visual results. All tested devices could be actuated by the DC control signal and the switch was released after the actuation voltage dropped to zero level.

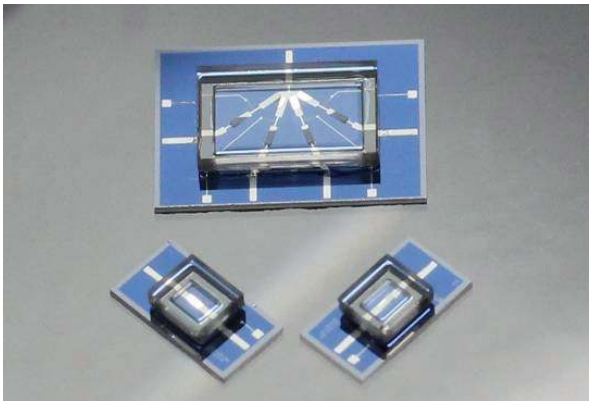

**Figure 8.** SPST and SP4T switch elements after final dicing process. No water was observed inside the cavity and the final testing was passed successfully.

### 2.3. RF Front-Ends

To reduce the interference between simultaneously transmitted data from several LEO satellites, it is planned to use a frequency division scheme. Each LEO satellite sends its data using different frequencies in the ISL band around 26 GHz. The maximum available bandwidth is 1 GHz, divided into 25 channels, each providing 36 MHz of bandwidth with a channel spacing of 40 MHz. All channels use the same type of circular polarization to reduce the complexity of the multifeed array and analog circuitry. However, supporting dual polarization is also possible. The main functions of the RF front-ends are to tune to the LEO satellite transmit frequency, amplify the received signal, filter out-of-band signals, and down convert it to 70 MHz center frequency, where it is handed over to the digital beam forming unit. The 70 MHz frequency was selected to have a wide range of commercially available components (e.g., SAW-filters). The receiver is based on the double superheterodyne concept (Fig. 9), which is the preferred topology in terms of image rejection and channel separation. The first intermediate frequency was selected to be in the 5.8 GHz ISM-band to minimize in-band mixing products and at the same time to take advantage of a great variety of components available for this frequency range.

A tunable local oscillator (LO) is used as the first mixer stage for channel selection. Thus, each receive channel is down converted to the same intermediate frequency band centered at 5.8 GHz. A subharmonically pumped mixer is selected for easier LO generation at half the LO frequency and less interference between LO and RF. Both signal paths need their individual first LO, since different receive

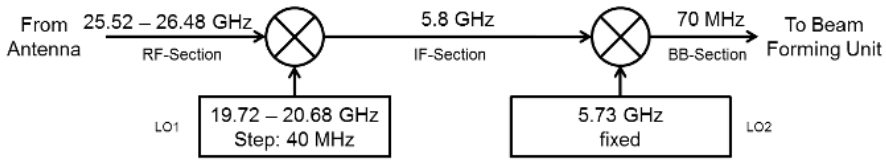


**Figure 9.** Block diagram of double superheterodyne receiver.

channels will be selected via serial command from the beamforming unit for each receiver path. The second LO generates a fixed frequency and is realized as a phase locked oscillator (PLO). Although the relatively small step size of 40 MHz at 26 GHz output could be easier realized using a fractional-N Phase Locked Loop (PLL) synthesizer, both LOs are designed as Integer-N PLL synthesizers to avoid fractional spurs in the passband, often associated with fractional-N PLL synthesizer architectures. Both LO synthesizers are phase locked to a built-in 100 MHz oven-controlled crystal oscillator (OCXO) providing frequency stability and an ultra-low phase noise 100 MHz signal for the phase detectors. To improve phase-noise of the synthesized LOs, an offset PLL architecture is employed for both LOs. A low phase noise 7.2 GHz auxiliary frequency is generated by multiplication of the 100 MHz OCXO output signal. Subtracting the auxiliary frequency from the LO outputs allows for phase detection at a lower frequency with smaller division ratios resulting in a better fine tunability and overall phase-noise, according to the 20 log(N)-law for the PLL in-band phase-noise, at the same time.

### 2.4. Digital Hardware

The digital hardware has to perform three different tasks which are depicted in Fig. 10: digital signal processing of the radio frequency input signals, calibration of the antenna array and receiver path and switching between different subarrays. For digitalization of the input signal and back conversion of the output signals, the system needs a number of analog-to-digital (ADC) and digital-to-analog (DAC) converters. The core unit is a field programmable gate array (FPGA), which performs the digital signal processing (DSP) tasks. The hardware is connected to the RF front-ends from which it takes analog input signals centered at 70 MHz.

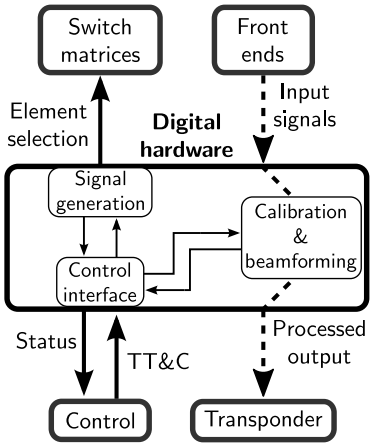


**Figure 10.** Interfaces of the digital hardware.

The output of the beamforming part is the beamformed signal in the analog domain with 70 MHz center frequency, feeding the satellite transponders. The structure of the RF-path is shown in Fig. 11. For beamforming, it is necessary to downmix the signals to the complex baseband. This is done in two steps. Due to the system clock frequency, the ADCs automatically perform bandpass sampling which leads to an intermediate frequency. Inside the FPGA the inputs are then mixed down to the base band, thereby extracting in-phase and quadrature component. After lowpass filtering to eliminate

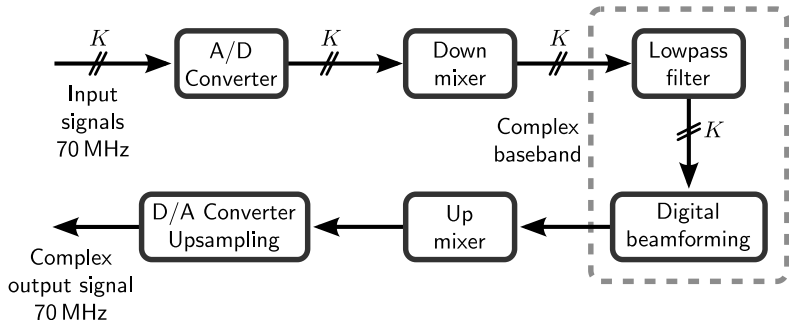


**Figure 11.** Flow chart of the RF-path inside the digital hardware.

higher mixing products, beamforming is applied. The resulting output signal is again upmixed in two stages: first by a numerically controlled oscillator (NCO) inside the FPGA, second in the DACs which also perform upsampling by a factor of four.

The variable signal path lengths introduced by the beam switching in combination with the very short wavelengths at Ka-band and high temperature changes in space require a permanent calibration of the receiver system. This must take into account the influences of the reflector, antenna array, switch matrices, front-ends and ADCs. To include all these effects, the calibration must be done inside the DSP unit. To avoid introducing more multiplication operations in the design, the calibration coefficients are included in the beamforming weights. The most accurate calibration can be achieved with an adaptive calibration algorithm. The chosen algorithm is based on the method of least squares (LMS) and uses its well-known filtering-and-update equations [25]. To actuate the switch matrices, it is necessary to generate a large number of control signals. Since the FPGA does not have enough output pins to support this directly, multiplexing is necessary. This is done by using a chain of shift registers. The advantage of this solution is that there can be as many registers in the chain as necessary. The signals can be serially created, put through the chain and are finally simultaneously forwarded to the switch matrix. Because loading many registers in sequence can take a considerable amount of time, several shorter shift register chains can also be used in parallel. Simulations show that tracking LEO satellites with the proposed antenna configuration requires reconfiguration of the switch matrix (changing of the active subarray) after several seconds or even minutes.

## 3. ANTENNA DEMONSTRATOR

A demonstrator showing the basic functionality of the antenna was built as a proof of concept of the proposed antenna. The demonstration system is composed of a reflector, a $4 \times 4$ multifeed array, a switch matrix based on RF MEMS switches, eight RF front-ends and a digital hardware unit. The demonstrator is capable to simultaneously receive signals from two movable sources using different frequency channels. Digital beamforming with four antenna elements for each beam is performed. Fig. 12 depicts a demonstration setup in which the received signal quality is measured using a vector signal analyzer.

Figure 13 shows a photograph of the realized demonstration system with graphical user interface of the controlling software.

### 3.1. Array-Fed Reflector

The reflector is built in a single offset configuration with a diameter of 60 cm, F/D ratio of 1.5 and an offset angle of 25°. It is fed by a $4 \times 4$ multifeed patch array with element distance of 10 mm. The reflector and the multifeed array are mounted on a special fixture that enables precise adjusting of all important parameters like focal length, tilt angle and rotation of the multifeed array. Thus, the influence of imperfect adjusting of the multifeed array can be measured. As the reachable scan volume with the $4 \times 4$ array is restricted to approximately $\pm 1°$, the position of the multifeed array can be precisely shifted along x-axis so that in the symmetry plane any scan angle up to $\pm 10°$ can be achieved.

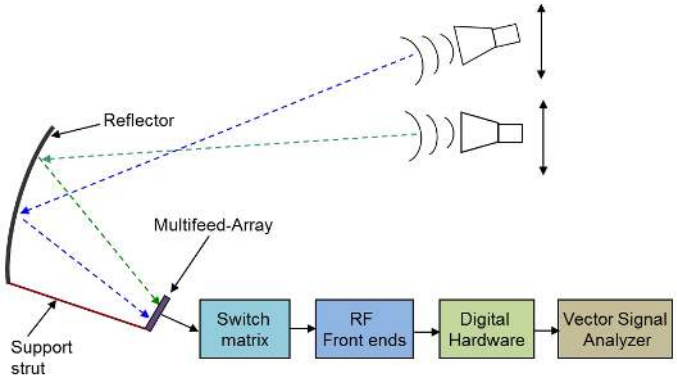


**Figure 12.** Schematic view of the demonstration setup.

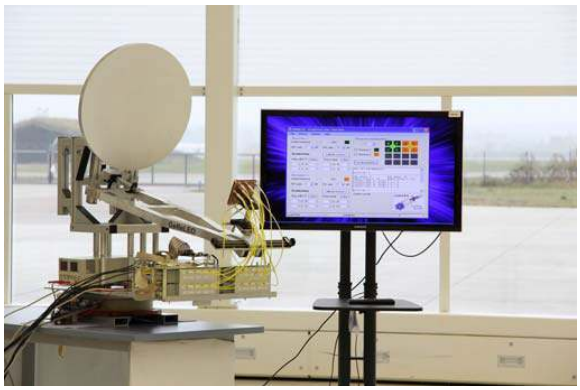

**Figure 13.** Photograph of the demonstration system.

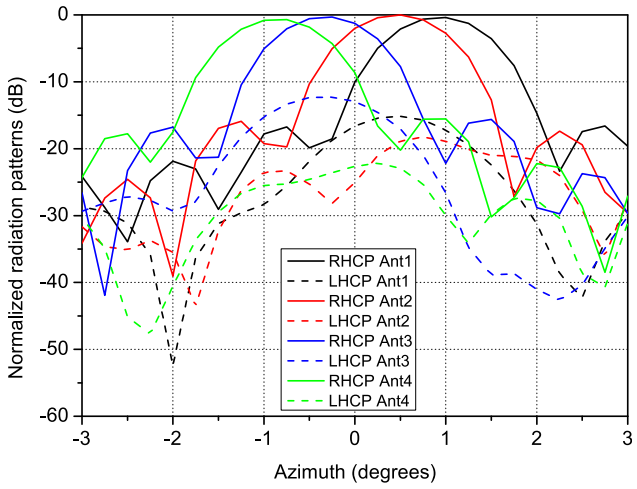


**Figure 14.** Measured radiation patterns of the reflector fed by single patches.

Scanning capabilities of the reflector were measured in a compact antenna test range of DLR for the case of feeding the reflector with only one patch antenna at a time. Fig. 14 shows the resulting radiation patterns in the symmetry plane, for feeds located in the upper row of the $4 \times 4$ array.

The $4 \times 4$ multifeed array was fabricated using Rogers RT/duroid 6002 high frequency laminates. As radiating elements, aperture coupled square patches were used. Circular polarization was obtained through exciting of two orthogonal modes using a 90° hybrid and two feed lines. As the application of antennas based on soft substrates is relatively new to space applications, some environmental tests were performed on the fabricated patch antennas/arrays. Vibration, shock and thermal-vacuum cycling were tested according to ECSS10-03A requirements [12]. All these tests were passed.

### 3.2. RF MEMS Switch Matrix

The switch matrix for the demonstration system must provide $16 \times 8$ switch functionality. Since $2 \times 2$ subarrays are used to receive each beam, only such combinations need to be realized. Removing unnecessary and redundant combinations allows for significant reduction of switch matrix complexity. The $4 \times 4$ array is built on a base of four $2 \times 2$ subarrays indicated in Fig. 15(a) by different colors and subscripts. Consequently, the design is reduced to four simple switch modules with four inputs and two outputs each, as depicted in Fig. 15(b). The demonstrator switch matrix was realized using commercially available RF MEMS SPDT switches. Key performance parameters are an insertion loss


(a) (b)

**Figure 15.** Concept of the switch matrix for the demonstration system. (a) Division on $2 \times 2$ subarrays. (b) Schematic view of a switch module.

between 7.0 dB and 8.5 dB, isolation between two channels of 50 dB, and input matching of 18 dB, all at 26 GHz. More detailed information on construction of the switch matrix and measured results can be found in [14].

### 3.3. RF Front-Ends

The realized demonstrator provides receive paths for two satellite signals. Each path consists of four similar front-ends and downconverters. The RF sections of the demonstrator system are actually made on Rogers RO3003 substrate using a soldered LNA. LOs are directly locked to the 100 MHz OCXO reference oscillator. Improvements of the system noise figure are expected by use of Al2O3 ceramic substrate with bonded chips in the RF-section. Use of offset-PLLs for LO frequency generation will lead to better phase-noise. The RF front-end is optimized for low noise figure (NF) of 2 dB at a maximum overall gain of approximately 60 dB within the front-end and downconverter stages. A 30 dB gain adjust range in the baseband section can be used, to accommodate different receive scenarios during the field tests. The system noise figure is dominated by the first low noise amplifier. For the demonstrator, a commercially available LNA with a noise figure of 1.9 dB was selected. IF-section and LOs are manufactured conventionally. All receiver sections are housed in milled aluminum cases for better isolation. Fig. 16 shows a measured output spectrum of RF front-end for a frequency sweep of $\pm 16$ MHz around 26 GHz.

### 3.4. Digital Hardware

The digital hardware for the demonstrator system is realized on a Lyrtech carrier board with a Virtex-4 FPGA. The board also provides eight ADCs and eight DACs. It is plugged into a host PC which facilitates the implementation of user interfaces and offers debug and analyzing possibilities for the FPGA design. The design supports two parallel beamforming units. The power consumption does not exceed 5.5 W. A graphical user interface (GUI) running on the host PC gives manual control over the system. It allows access to element configuration switching, calibration process and manual beamforming operations. In the demonstrator, 80 logic signals are necessary to control the switch matrices. The switching operation is triggered by the FPGA. Additional details about the digital hardware of the demonstration systems can be found in [15].

### 3.5. Measurements of the Whole Demonstration System

Many comprehensive tests were performed with the whole demonstration system. Signals from two movable sources could be received in parallel. The influence of beam switching, adaptive calibration and digital beamforming on the received signal could be measured. The tests were performed not only with CW signals but also video transmission using DVB-S modems was realized. Fig. 17 depicts the measured output spectrum of the whole signal chain. To suppress the undesired mirrored frequency bands, analog bandpass filters can be used.

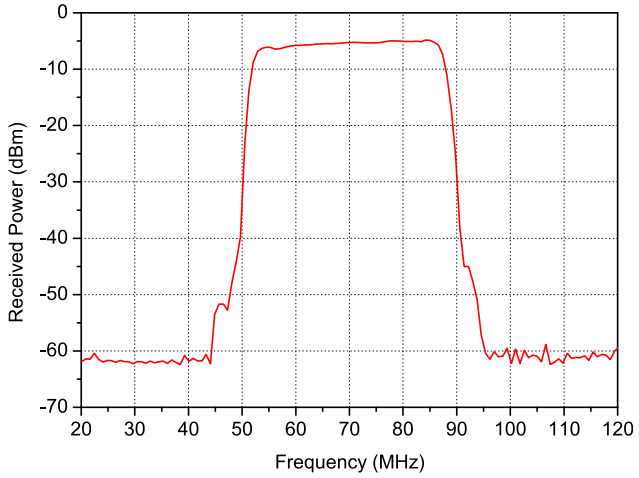


**Figure 16.** Output spectrum of the RF front-ends for a ±16 MHz frequency sweep around 26 GHz.

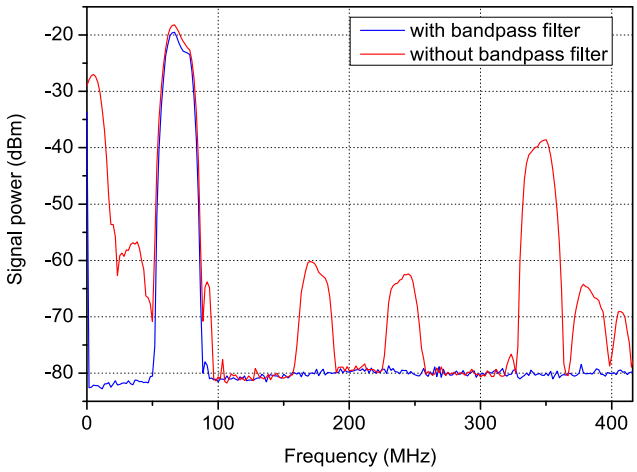


**Figure 17.** Output spectrum for a ±15 MHz frequency sweep around 26 GHz using the signal chain.

## 4. CONCLUSIONS

In this paper a concept and the development of key components of a satellite multiple-beam antenna for high-rate data relays have been presented. The conducted numerical simulations and measurements revealed that the proposed antenna system including the deployment of microstrip technology for the multifeed array meets the performance requirements for its application. The development of a large switch matrix using RF MEMS switches based on modular architecture has been described and the packaging of these switches has been addressed. With the help of a demonstration system the basic antenna functionality and the proper interaction of various antenna parts were substantiated. Before the antenna can be deployed on a GEO satellite additional investigations are required, particularly in-orbit-validation of the critical components: RF MEMS switches and active antennas built in microstrip technology. In a current project it is planned to validate these components on a German scientific small-GEO satellite Heinrich Hertz that is supposed to be launched in 2018.

## ACKNOWLEDGMENT

This work was supported in part by the Space Administration of the German Aerospace Center (DLR) on behalf of the Federal Ministry of Economics and Technology through the "GEO data relays for low earth orbit satellites GeReLEO" project under contract No. 50 YB 0907 (0911).

## REFERENCES

1. Yuan, J., D. Yang, and X. Sun, "Single access antenna pointing control system design of TDRS," *1st Intern. Symp.on Systems and Control in Aerospace and Aeronautics*, Harbin, Jan. 2006.
2. Galindo-Israel, V., S. Lee, and R. Mittra, "Synthesis of a laterally displaced cluster feed for a reflector antenna with application to multiple beams and contoured patterns," *IEEE Trans. Antennas Propag.*, Vol. 26, No. 2, 220–228, Mar. 1978.
3. Lier, E. and R. Melcher, "A modular and lightweight multibeam active phased receiving array for satellite applications: design and ground testing," *IEEE Trans. Antennas Propag.*, Vol. 51, No. 1, 80–90, Feb. 2009.
4. Zaghloul, A. I., R. K. Gupta, E. C. Kohls, and O. Kilic, "Design and performance assessment of active phased arrays for communications satellites," *IEEE International Conference on Phased Array Systems and Technology*, 197–201, Dana Point, Ca., May 2000.

5. Seong, N., C. Pyo, J. Chae, and C. Kim, "Ka-band satellite active phased array multi-beam antenna," *IEEE 59th Vehicular Technology Conf.*, Vol. 5, 2807–2810, Milan, Italy, May 2004.
6. Litva, J. and T. K.-Y. Lo, *Digital Beamforming in Wireless Applications*, Artech House, 1996.
7. Haymann, D. B., T. S. Bird, K. P. Esselle, and P. J. Hall, "Experimental demonstration of focal plane array beamforming in a prototype radiotelescope," *IEEE Trans. Antennas Propag.*, Vol. 58, No. 6, 1922–1934, Jun. 2010.
8. Duggan, J. and P. McLane, "Adaptive beamforming with a multiple beam antenna," *IEEE International Conference on Communications*, 395–401, Atlanta, Ga., Jun. 1998.
9. Greda, L. A., B. Knuepfer, M. V. T. Heckler, J. S. Knogl, H. Bischl, A. Dreher, and C. Guenther, "A satellite multibeam antenna for high-rate data relays," *32nd ESA Workshop on Antennas for Space Applications*, ESA/ESTEC, Noordwijk, the Netherlands, Oct. 2010.
10. Ziegler, V., A. Stehle, G. Georgiev, B. Schoenlinner, U. Prechtel, H. Seidel, U. Schmid, and J. Hartmann, "SP48T module architecture and RF-MEMS multi-throw switches for a multi-beam antenna measurement set-up at K- and Ka-band," *39th European Microwave Conference*, Rome, Italy, Apr. 2011.
11. Greda, L. A. and A. Dreher, "Beamforming capabilities of array-fed reflector antennas," *European Conference on Antennas and Propagation*, Rome, Italy, Apr. 2011.
12. Greda, L. A., Z. Katona, B. Knuepfer, W. Elmarissi, and A. Dreher, "Development of a satellite multibeam antenna for high-rate data relays: current status," *33rd ESA Workshop on Antennas*, ESA/ESTEC, Noordwijk, the Netherlands, Oct. 2011.
13. Siegel, C., V. Ziegler, B. Schoenlinner, U. Prechtel, and H. Schumacher, "Simplified RF-MEMS switches using implanted conductors and thermal oxide," *36th European Microwave Conference*, 1735–1738, Manchester, UK, Sep. 2006.
14. Figur, S. A., E. Meniconi, U. Prechtel, V. Ziegler, B. Schoenlinner, R. Sorrentino, and L. Vietzorreck, "Design and characterization of a simplified planar $16 \times 8$ RF MEMS switch matrix for a GEO-stationary data relay," *European Microwave Week*, Amsterdam, the Netherlands, Oct. 2012.
15. Greda, L. A., A. Winterstein, M. Brueck, and A. Dreher, "Demonstrator concept for a satellite multiple-beam antenna for high-rate data relays," *6th Advanced Satellite Multimedia Systems Conference*, Baiona, Spain, Sep. 2012.
16. Jorgensen, R., P. Balling, and W. J. English, "Dual offset reflector multibeam antenna for international communications satellite applications," *IEEE Trans. Antennas Propag.*, Vol. 33, No. 12, 1304–1312, Dec. 1985.
17. Chandler, C., L. Hoey, D. Nixon, T. Smigla, A. Peebes, and M. Em, "Ka-band communications satellite antenna technology," *20th AIAA International Communication Satellite Systems Conference and Exibit*, Montreal, Canada, May 2002.
18. Malik, D. P. S., J. M. Eskell, and M. H. Skeen, "Microstrip patch antennas for space application," *IEE Colloquium on Satellite Antenna Technology in the 21st Century*, 9/1–9/5, London, UK, Jun. 1991.
19. Diodato, N. (ed.), *Satellite Communications*, 367–394, Scivo Inc., India, 2010.
20. Ramm, P., J. J. Q. Lu, and M. V. Taklo, *Handbook of Wafer Bonding*, Wiley-VCH, 2012.
21. Lee, K. Y., et al., "Micromachining applications of a high resolution ultrathick photoresist," *10th International Symposium on RF MEMS and RF Microsystems*, Trento, Italy, Jul. 2009.
22. http://www.radiantmems.com.
23. Seki, T., et al., "RF-MEMS contact switch technology in OMRON," *Journal of Vacuum Science & Technology B: Microelectronics and Nanometer Structures*, Vol. 13, No. 6, 3012–3016, Nov. 1995.
24. http://www.wispry.com.
25. Haykin, S. S., *Adaptive Filter Theory*, Prentice Hall, 2002.